Journal of sustainable food, water, energy and environment

Deposition parameters influencing structural and optical properties of SnO_2/TiO_2 thin films for UV photodetector environmental monitoring applications

M. A. Awad[1], Abdalrahman M. Rayan[1], S.H. Mohamed[1,2]

[1]Physics Department, Faculty of Science, Sohag University, 82524 Sohag, Egypt
[1]Falculty of Graduate Studies and Environmental Research, Sohag University, 82524 Sohag, Egypt

Received: 22 June. 2025, Revised: 8 July. 2025, Accepted: 21 July. 2025 Published online 31 July. 2025

Abstract: SnO_2 thin films were synthesized on pre-sputtered TiO_2 layers using a thermal chemical vapor deposition technique under two deposition parameters: a high oxygen flow rate (200 sccm; sample 1) and a long deposition time (180 min; sample 2). The influence of deposition parameters on the overall properties was systematically investigated using different analytical techniques. X-ray diffraction revealed high crystalline quality with three intermixed phases - SnO_2, TiO_2 and $Ti_{26.72}O_{48}$ for sample 2, in contrast to those synthesized at 200 sccm (sample 1). Morphological analysis supports the structural findings by revealing a uniform and denser microstructure in thin films prepared with moderate oxygen flow (75 sccm) but longer deposition time 180 min. Optical measurements showed moderate transparency under both conditions, with slightly lower transparency (60%), a higher refractive index (3.03) and a wider optical band gap (3.64 eV) in the thin films of sample 2. The static dielectric constant (ε_0) obtained from the theoretical Penn model and semi empirical Adachi relation showed close proximity. These findings suggest the promise of using SnO_2/TiO_2 thin films prepared under extended deposition time (180 min) to be valuable in applications such as UV photodetectors for environmental monitoring.

Keywords: SnO_2/TiO_2; long deposition parameters; high oxygen flow rate; static dielectric constant; Penn model; Adachi relation

1. Introduction

Metal oxide thin films have been extensively studied for several decades due to their numerous applications in various fields such as photodetectors [1, 2], gas sensors [3], photocatalysis [4], solar cells [5], etc. These widespread applications derived from their unique advantages, such as high optical transparency [6], good electrical conductivity [6], and high thermal stability [7]. Among these metal oxides, SnO_2 and TiO_2 are of particular interest. Where their combination in heterostructure offers a strategy to enhance their performance through combining the advantages of the two oxides. The usage of TiO_2 as a buffer substrate improves adhesion of the epitaxial layer, influences the crystal orientation, and enhances charge separation that is beneficial for applications such as UV photodetectors, photocatalysis, and gas sensors [8-10]. The performance of SnO_2/TiO_2 thin films is greatly dependent on deposition parameters, which significantly affect crystallinity, morphology, optical and electrical characteristics.

In this study, SnO_2 thin films were deposited on pre-sputtered TiO_2 layers using the thermal chemical vapor deposition technique under two different experimental conditions: a high oxygen flow rate of 200 sccm and an extended deposition time of 180 min. The aim was to compare the impact of deposition parameters on overall properties of the prepared films. The results indicated that thin films prepared at extended deposition times (180 min) exhibited superior characteristics, such as high crystalline quality, uniform and dense surface morphology, good optical, electrical, and dielectric properties. This highlights their potential usage in applications such as UV photodetectors, photocatalysis, and semitransparent electrodes in solar cells.

2. Experimental

Thin films of SnO_2/TiO_2 thin films were synthesized in two step processes using DC magnetron sputtering followed by CVD technique. Before deposition, Si and glass substrates were ultrasonically cleaned in an acetone for 15 min followed by deionized water and then they are carefully dried. In the sputtering system, the TiO_2 buffer layer was carefully grown using Ti target under oxygen (O), nitrogen (N) and argon (Ar) flow rate of 15, 60 and 25 sccm,

* Corresponding author E-mail: arwamadeha@yahoo.com Print ISSN 3062-5513 Online ISSN 3062-5521

respectively. Where these thin films were then used as substrate for the subsequent growth of SnO_2 thin films. The deposition of SnO_2 in CVD technique was under two different experimental conditions as shown in Table 1. At the end of each experiment, the furnace was left to cool naturally to room temperature while maintain the Ar flow to protect the rapid oxidation.

The thicknesses of the SnO_2/TiO_2 thin films were measured utilizing Form Talysurf 50 profilometer. The obtained values are listed in Table 1. The produced SnO_2/TiO_2 thin films were subjected to various characterization techniques to analyze their structural, morphological, optical and electrical properties. X-ray diffraction (XRD) was used to analyze the crystal structure using Bruker D8-Advanced X-ray diffractometer. The morphological and compositional analysis were conducted using scanning electron microscope (SEM) and energy dispersive analysis of X-ray (EDAX) (JEOL, Japan), respectively. The optical properties were measured in the wavelength range 200-1200 nm using spectrophotometer.

Table 1: CVD preparation conditions and thicknesses obtained from Form Talysurf 50 profilometer.

Sample	Temp. (°C)	Ar flow rate (sccm)	O_2 flow rate (sccm)	Deposition Time (min)	Thickness of SnO_2/TiO_2 (nm)
Sample 1	400	200	200	90	310/103
Sample 2	400	200	75	180	301/103

3. Results and discussions

3.1 Microstructural analysis

The XRD of SnO_2/TiO_2 thin films at an oxygen flow rate of 200 sccm (Fig. 1a) demonstrates a very low crystalline nature, where only two distinct planes of (011) and (222) associated with the TiO_2 phase (COD 5000223) [11] and the $Ti_{26.72}O_{48}$ phase (COD database code: 9014505) are observed. The absence of SnO_2 peaks although deposition suggests the amorphous distribution with no long-range structural order. In contrast, the crystal structure of SnO_2/TiO_2 deposited with 75 sccm and for 180 min (Fig. 1b) reveals the formation of a polycrystalline structure, where all diffracted peaks are predominantly related to the rutile SnO_2 phase (COD 1534785) with preferred orientation along the (200) plane. This preferred orientation indicates the anisotropic growth of SnO_2 phase that reduces charge carrier scattering and enhances the electrical and overall properties of the prepared thin films [12].

The crystallite size (D) of SnO_2/TiO_2 thin films was calculated using the Scherrer equation [13], given through

$$D = \frac{K\,\lambda}{\beta\,cos\theta} \qquad (1)$$

where λ is the x-ray wavelength equal to 1.54060 Å, β is the FWHM, θ is the Bragg angle in radians, and K is the shape factor with a value usually ~ 0.9. Based on the (222) diffraction planes at 2θ = 31.78° and FWHM of 0.12686°, the crystallite size of thin films prepared at oxygen flow rate of 200 sccm is 65.11 nm. On the other hand, for thin films deposited at 180 min (Fig. 1b), the crystallite size was calculated using the (200) diffraction planes. Where the calculated crystallite size was 48.75 nm using 2θ of 37.84° and FWHM of 0.17237°. Worth noting, crystallites size from XRD shows an apparent contradiction when compared with the crystal structure depicted in Fig. 1a and 1b. The reason is that the Scherrer equation estimates crystallite size only from a specific crystallographic plane. Moreover, it is important to clarify that higher crystallinity doesn't mean larger crystallite size, where thin films composed of numerous small, well-ordered crystallites can produce sharp and intense XRD peaks, which in turn produce relatively small crystallites size. On contrary, in Fig. 1a the presence of localized large crystallites, particularly from (222) planes, lead to large crystallites size even though the overall film crystallinity is lower.

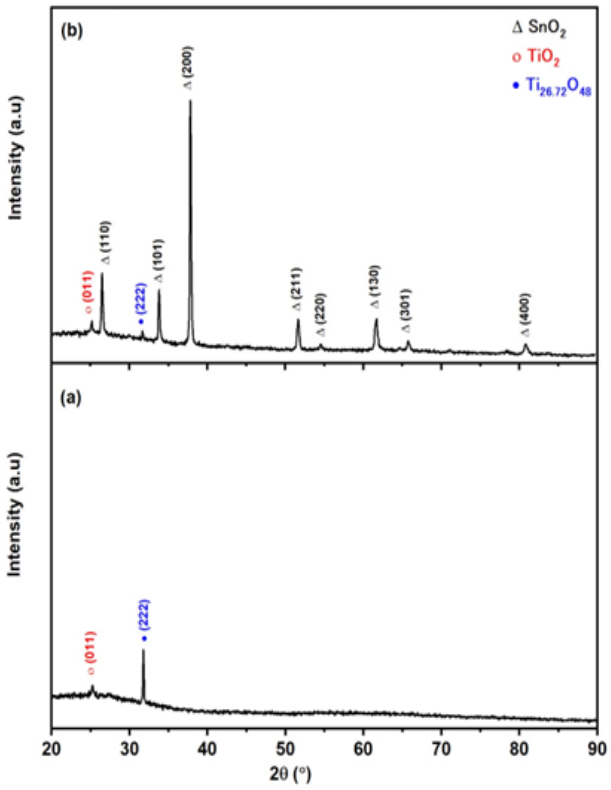

Fig. 1: The XRD of SnO_2/TiO_2 thin films at an oxygen flow rate of 200 sccm, sample 1, (a) long deposition time 180 min, sample 2, (b).

Fig. 2 compare the surface morphology analysis of SnO2/TiO2 thin films of sample 1 (Fig. 2a) and sample 2 (Fig, 2b). Clearly, randomly distributed and loosely packed nanocrystallites are observed at high oxygen flow rate (sample 1) which are not achieved at long deposition time (sample 2), where more dens and grains packing are observed. These results of surface morphology support the XRD results depicted in Fig. 1.

The EDAX spectrum of sample 1 is shown in Fig. 2c and it confirms the presence of Sn, O, and Ti peaks whereas Cl peaks originate from the residual chloride precursor. On the other hand, in Fig. 2d (sample 2), the Cl peaks are not observed due to their removal at long deposition time (180 min).

3.2 Optical and dielectric properties

The optical behavior of SnO_2/TiO_2 thin films (Fig. 3) is strongly dependent on their structural and morphological properties. Where thin film deposited at a high oxygen flow rate (Sample 1) exhibits lower than expected transparency (~ 70% in the visible to near IR region). This reduction is attributed to the poor crystallinity of the as grown thin films (Fig. 1a), that increases light scattering [14]. These structural inhomogeneities increase light scattering and surface reflectance [14], especially in the visible spectral range. On the other hand, the thin films deposited for longer deposition time (sample 2) shows relatively low transparency (~ 60%) despite the high crystal ordering. The reason relies on increasing film thickness that increased the light polarization [15].

The optical band gap was calculated using the direct allowed transition of the Tauc equation [16] (Fig. 4) given by

$$(\alpha h\nu)^2 = \beta(h\nu - E_g) \qquad (2)$$

where α is the absorption coefficient and hν is the photon energy. For SnO_2/TiO_2 deposited under a high oxygen flow rate (sample 1), the calculated E_g value was 3.58 eV. In contrast, the thin films deposited with a longer deposition time (sample 2) and a moderate oxygen flow rate (75 sccm) possess a higher optical band gap value (E_g = 3.64 eV). The improved crystallinity, which reduced the defect states and shifted the absorption to higher energies, is responsible for this increase [6].

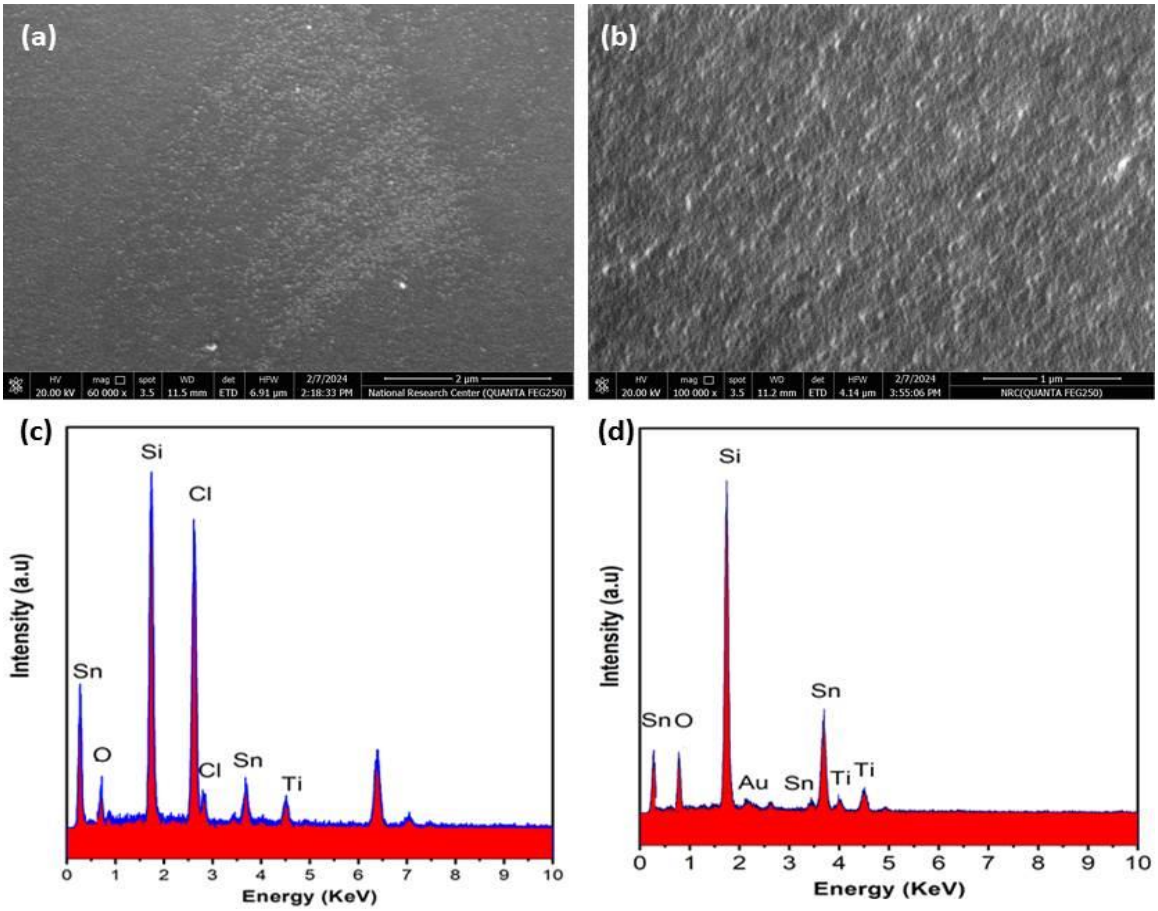

Fig. 2: SEM images of (a) sample 1 and (b) sample 2. EDAX spectra of (c) sample 1 and (d) sample 2.

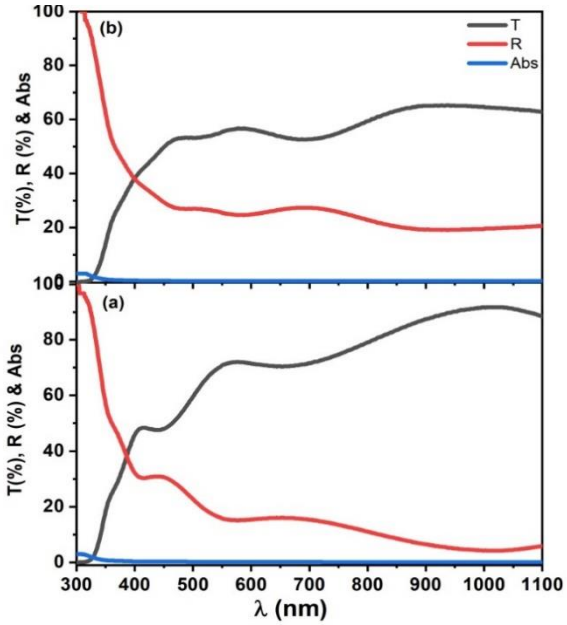

Fig. **3:** Optical transmittance, reflectance and absorbance of (a) sample 1 and (b) sample 2.

Fig. 5 depicts the refractive index (n) and extinction coefficient (k) of SnO_2/TiO_2 thin films deposited at a high oxygen flow rate (Fig. 5a; sample 1) and at a long deposition time (Fig.5b; sample 2). The thin films deposited for a long deposition time show a higher refractive index (n = 3.03 at 600 nm) compared to those deposited at a high oxygen flow rate (2.36 at 600 nm). This increase is attributed to enhanced crystallinity and denser microstructure that increases light polarization [15]. On regard to the extinction coefficient (k), both films show high value in the UV range as a result of electron transfer from the valence band to the conduction band. As the wavelength increases, the extinction coefficient decreases for both condition (sample 1 and sample 2). The slightly high k values observed for the films with longer deposition time, especially in the NIR region, suggest increased optical losses due to the increase of free carrier absorption [17-19].

In order estimate the dielectric properties of SnO_2/TiO_2 thin films at constant electric field, the static dielectric constant ε_0 was approximated using the theoretical Penn model [20] for wide band gap semiconductors using the relation

$$\varepsilon_0 = 1 + (\frac{\hbar\omega_p}{E_g})^2 \qquad (3)$$

where E_g is the optical band gap and ω_p is the plasma frequency and $\hbar$ is the reduced Planck constant. For many wide band gap semiconductors, the plasma energy ($\hbar\omega_p$) is typically taken as 9- 10 eV [21,22]. Using the value of 10 eV and the band gap energy of 3.58 and 3.64 eV for SnO_2/TiO_2 thin films deposited at high oxygen flow rate (sample 1) and long deposition time (sample 2), respectively, yields dielectric constant values of 8.81 and 8.55, respectively. These values reflect the strong polarizability of the prepared thin films, where their values are higher than that was reported for single phase of SnO_2.

The static dielectric constant of SnO_2/TiO_2 thin films is also calculated using semi-empirical Adachi relation [22] given through,

$$\mathcal{E}_0 = 18.52 - 3.08\ E_g \qquad (4)$$

yielding values of 7.49 and 7.31 for thin films prepared at high oxygen flow rate (sample 1) and long deposition time (sample 2).

Comparing the static dielectric constant calculated using Penn model and Adachi relation shows close agreement and are consistent with the values reported in the literature [6,24].

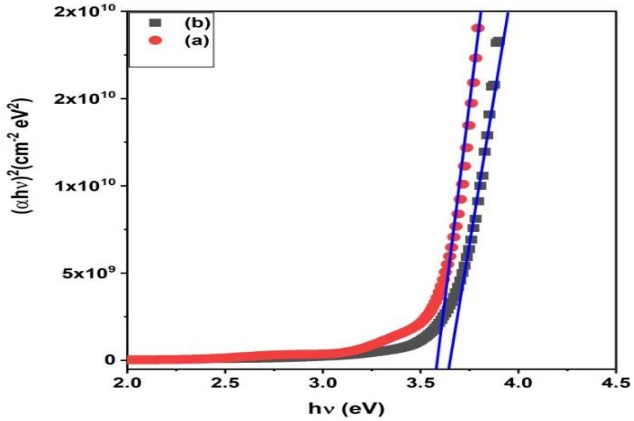

Fig. 4: $(\alpha h\nu)^2$ versus $h\nu$ plots.

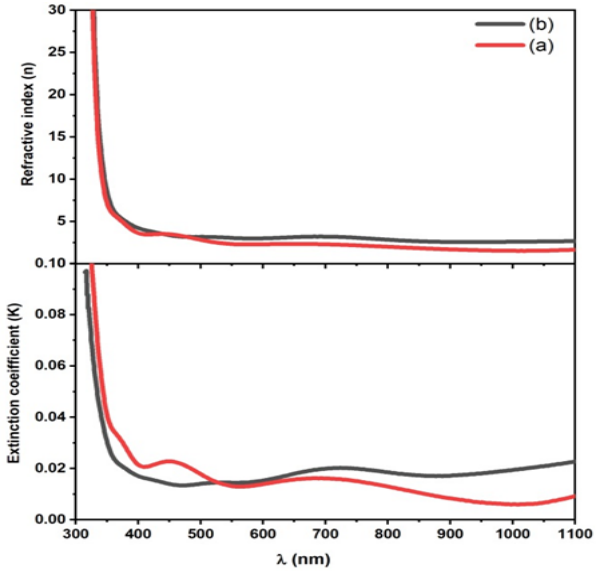

Fig. 5: refractive index and extinction coefficient of (a) sample 1 and (b) sample 2.

4. Conclusion

SnO_2 thin films is successfully deposited on TiO_2 thin films using CVD technique under two different conditions of high oxygen flow rate (sample 1) and long deposition time (sample 2), while maintaining constant furnace temperature and Ar flow rate. High crystalline quality and compacted uniform microstructure were obtained for thin film prepared at long deposition time which is not achieved at high oxygen flow rate. The static dielectric constant estimated via both the Adachi and the Penn model showed close agreement. These finding suggests the possibility of using SnO_2/TiO_2 thin films prepared at long deposition time in applications such as UV photodetector environmental monitoring.

5. References

[1] T. Zhai, X. Fang, M. Liao, X. Xu, H. Zeng, B. Yoshio, D.J.S. Golberg, A comprehensive review of one-dimensional metal-oxide nanostructure photodetectors, Sensors vol. 9, pp. 6504-6529, 2009.

[2] M. A. Awad, M. Shaban, M. Rabia, The efficiency of M (M= Li, Na, or Cs) doped CdS nanomaterials in optoelectronic applications, Int. J. Energy Res. Vol. 46 pp. 8443-8451, 2022.

[3] Y. Yoon, P. L. Truong, D. Lee, S. H. Ko, Metal-oxide nanomaterials synthesis and applications in flexible and wearable sensors, ACS Nanosci. Au vol. 2, 64−92, 2022.

[4] D. Nunes, A. Pimentel, R. Branquinho, E. Fortunato, R.J.C. Martins, Metal oxide-based photocatalytic paper: A green alternative for environmental remediation, Catalysts vol. 11, pp. 504, 2021.

[5] H. Soonmin, A review of metal oxide thin films in solar cell applications, Int. J. Thin Films Sci. Technol. vol. 11, pp. 37-45, 2022.

[6] M. A. Awad, E.R. Abaza, E.R. Shaaban, Optimizing the conditions to synthesize transparent conductive SnO_2 thin films for optoelectronic applications, Surf. Interfaces vol. 69, pp. 106734, 2025.

[7] M. A. Awad, E. M. M. Ibrahim, A, M. Ahmed, Synthesis and thermal stability of ZnO nanowires, J. Therm. Anal. Calorim. Vol. 117, pp. 635-642, 2014.

[8] K. Maver, I. Arčon, M. Fanetti, S. Al Jitan, G. Palmisano, M. Valant, U.L. Štangar, Improved photocatalytic activity of SnO_2-TiO_2 nanocomposite thin films prepared by low-temperature sol-gel method, Catal. Today vol. 397-399, pp. 540-549, 2022.

[9] M.J. Jeong, S.W. Lee, Y. Shin, J.-H. Choi, J.-H.J.S. Ahn, Implementation of rutile-TiO_2 thin films on TiN without post-annealing through introduction of SnO_2 and its improved electrical properties, Surf. Interfaces vol. 42, pp. 103420, 2023.

[10] B. Yadav, N. Verma, S.J.O. Singh, L. Technology, Nanocrystalline SnO_2–TiO_2 thin film deposited on base of equilateral prism as an opto-electronic humidity sensor, Opt. Laser Technol. vol. 44, pp. 1681-1688, 2012.

[11] S. Sönmezoğlu, A. Arslan, T. Serin, N. Serin, The effects of film thickness on the optical properties of TiO_2–SnO_2 compound thin films, Physica Scripta vol. 84, pp. 065602, 2011.

[12] V. Consonni, G. Rey, H. Roussel, B. Doisneau, E. Blanquet, D.J. Bellet, Preferential orientation of fluorine-doped SnO_2 thin films: The effects of growth temperature, Acta Mater. vol. 61, pp. 22-31, 2013.

[13] A. Monshi, M.R. Foroughi, M.R. Monshi, engineering, Modified Scherrer equation to estimate more accurately nano-crystallite size using XRD, World J. Nano Sci. Eng. vol. 2, pp. 154-160, 2012.

[14] M. A. Awad, M.J.A.P.A. Rabia, Optimal temperature and Mn content for enhancing optical properties and inducing room temperature ferromagnetism of Mn doped In_2O_3 nanocubes, Appl. Phys. A vol. 128, pp. 225, 2022.

[15] M. A. Awad, M. Rabia, The bimetallic synthesis of TeO_2–Sb_2O_4 thin films for optoelectronic applications, Ceram. Int. vol. 49, pp. 37340-37348, 2023.

[16] Ł. Haryński, A. Olejnik, K. Grochowska, K.J. Siuzdak, A facile method for Tauc exponent and corresponding electronic transitions determination in semiconductors directly from UV–Vis spectroscopy data, Opt. Mater. vol. 127, pp. 112205, 2022.

[17] M. A. Awad, A. H. Aly, Experimental and theoretical studies of hybrid multifunctional $TiO_2/TiN/TiO_2$, Ceram. Int. vol. 45, pp. 19036-19043, 2019.

[18] S.H. Mohamed, K.M. Al-Mokhtar, Characterization of Cu_2O/CuO nanowire arrays synthesized by thermal method at various temperatures, Appl. Phys. A vol. 124, pp. 493, 2018.

[19] H. A. Mohamed, H. M. Ali, S. H. Mohamed and M. M. Abd El-Raheem, Transparent conducting ZnO-CdO thin films deposited by e-beam evaporation technique, Eur. Phys. J. Appl. Phys. vol. 34, pp. 7-12, 2006.

[20] A.J. Sharma, Size-dependent energy band gap and dielectric constant within the generalized Penn model applied to a semiconductor nanocrystallite, J. Appl. Phys. vol. 100, pp. 084301, 2006.

[21] R. Ravichandran, A.X. Wang, J.F. Wager, Solid state dielectric screening versus band gap trends and implications, Opt. Mater. vol. 60, pp. 181-187, 2016.

[22] N. Ravindra, P. Ganapathy, J.J. Choi, Energy gap–

refractive index relations in semiconductors–An overview, Infrared Phys. Technol. vol. 50 pp. 21-29, 2007.

[23] S. Adachi, Properties of semiconductor alloys: group-IV, III-V and II-VI semiconductors, John Wiley & Sons 2009.

[24] M.A. Yıldırım, The effect of copper concentration on structural, optical and dielectric properties of $Cu_xZn_{1-x}S$ thin films, Opt. Commun. vol. 285, pp. 1215-1220, 2012.